SCOPE | SAUDI INTERNATIONAL CONFERENCE ON NUCLEAR POWER ENGINEERING

Proceedings of SCOPE
13-15 Nov. 2023 – KFUPM
Paper 23132

Hybrid Microwave Sintering of Yttria Stabilized Zirconia

Morsi M. Mahmoud[1,2]
[1]Mechanical Engineering Department, College of Engineering and Physics.
[2]Interdisciplinary Research Center for Advanced Materials.
King Fahd University of Petroleum and Minerals, Dhahran, 31261, Saudi Arabia.
morsimahmoud@kfupm.edu.sa
Mohammed Arif[1]
[1]Mechanical Engineering Department, College of Engineering and Physics,
King Fahd University of Petroleum and Minerals, Dhahran, 31261, Saudi Arabia.
g202215340@kfupm.edu.sa
Zuhair M. Gasem[1,2]
[1]Mechanical Engineering Department, College of Engineering and Physics.
[2]Interdisciplinary Research Center for Advanced Materials.
King Fahd University of Petroleum and Minerals, Dhahran, 31261, Saudi Arabia.
zuhair@kfupm.edu.sa

Abstract – *Sintering of 7-8 wt.% yttria-stabilized zirconia (8 YSZ) was investigated using hybrid microwave (HMW) processing. HMW heating offers several advantages over regular conventional sintering methods such as but not limited to shorter processing times, more energy saving, faster ramp rate, homogenous volumetric heating and improved materials properties. Moreover, HMW offers a more homogenous and uniform heating profile than stand-alone pure microwave processing for such poor microwave absorber materials with low-dielectric contents, such as 8YSZ. 8 YSZ is a typical ceramic material that is being used in many state-of-the-art high-temperature applications such as thermal barrier coating (TBC). Commercial 8 YSZ powder was investigated in the current study where the powder was pressed and molded into green body disk using uniaxial press before it was later heated and sintered using HMW processing. A commercial hybrid microwave furnace was used during the sintering experiments using 2.45 GHz microwave frequency combined with conventional heating at the same cavity. 8 YSZ prepared green disks were heat-heated at 3 different temperatures: 1350 ºC, 1400 ºC and 1450 ºC using the same holding time of 2 hours before they were allowed to cool down to room temperature. The HMW sintered disks were characterized using X-ray diffraction (XRD) and scanning electron microscopy (SEM). The crystal size of HMW heated samples was calculated to be around 46-49 nm using Scherrer equation. Furthermore, SEM micrographs of the HMW heat-treated samples showed the typical sintered microstructure and grain boundaries. The phases evolution and the microstructural changes behavior of 8 YSZ during HMW processing were discussed. HMW processing was used successfully to sinter 8 YSZ samples where the transformation of the stable tetragonal (t-ZrO_2) phase into monoclinic (m-ZrO_2) phase was suppressed due to the formation of huge number of oxygen vacancies during HMW processing where the cubic (c-ZrO2) phase was stabilized due to that generated vacancies. HMW was slowing down the undesired martensite transformation which is usually associated with microcracks that leads to lower mechanical properties. Hybrid microwave processing is considered as a promising technique to sinter YSZ materials.*

Keywords: Hybrid microwave (HMW) processing, Sintering, Yttria-stabilized zirconia (YSZ), microstructure

I. Introduction

To cope with energy shortage and environmental issues, ceramists have directed their efforts and attention towards advanced rapid sintering, environmentally friendly and more energy saving techniques that are going to be suitable alternatives to the conventional used traditional methods[1, 2]. Rapid sintering processes, such as microwaves (MW), were explored since the early interest in MW sintering of ceramics[3-5]. MW sintering is a fast-sintering technique that offers the benefit of being a pressure-less process in addition to the other advantages such as: more energy saving, faster heating ramp, more uniform volumetric heating and improved material properties when compared with conventional heating [6, 7].

During MW sintering, the material molecules are directly interacting with the alternating electric and/or

magnetic electromagnetic fields, resulting in large number of defects and hence enhanced diffusion and kinetics rates that results in improved properties[8]. At room temperature (RT), materials can be classified into good, partially or poor MW absorbers depending on their dielectric and magnetic properties[9]. For poor MW absorbers materials such as ceramics, a hybrid microwave processing (HMW) technique had been developed[10]. HMW refers to the combination of MW energy and other conventional energy such as convection, infrared, and conventional heating in order to enhance the volumetric heating pattern of such poor MW absorbers materials.

At RT, zirconia (ZrO_2), as a typical ceramic material, has a monoclinic crystal structure that can undergo during heating into the well-known martensitic transformation into the tetragonal phase at ~ 1170 °C with around 3-4% of volume change in the unit cell[11]. Moreover, it can be stabilized in that tetragonal phase at a temperature range between 1170 °C and 2370 °C[12]. Finally, it can transform into another higher temperature cubic phase up to the melting point of ZrO_2 at ~2715°C[13]. Due to zirconia unique characteristics and applications, the high temperature phases can be stabilized at RT by adding different oxides and alloying elements such as but not limited to calcia (CaO), magnesia (MgO), and yttria (Y_2O_3)[14].

Yttria-stabilized zirconia (YSZ) is composed of two ceramics oxides, ZrO_2 and Y_2O_3, in which the latter is added as a dopant with different percentages in order to stabilize the high temperature phases at RT[15, 16], as shown in figure 1 of ZrO_2-Y_2O_3 phase diagram[11, 17]. The three (3) possible phases of zirconia with its space groups information are shown in table 1[11].

7–8 wt% Y_2O_3 which is equivalent to 3.8–4.4 mol% Y_2O_3 is denoted in this study as 8YSZ. It is considered as a current state-of-the-art thermal barrier coating (TBC) material and being used in wide high temperature applications due to its several advantages such as: higher melting point (~2800 °C), higher thermal expansion coefficient (CTE) (~10×10^{-6}/°C) with closer match to Ni-based superalloys (~12×10^{-6}/°C) at RT, lower tendency of crack-induced tetragonal (t) to monoclinic (m) martensitic transformation during cooling to RT, higher toughness than its corresponding cubic phase and finally higher chemical-phase-mechanical stability in corrosive high-temperature environment[18].

The crystal structure of the partially-stabilized 8YSZ material is related to tetragonal family with a space group: $P4_2/nmc$ (#137 -1), as shown in figure 2, with the lattice parameters shown in Table 2[19]. As shown in figure 2, zirconia (ZrO_2) crystallizes in this tetragonal $P4_2/nmc$ space group where Zr^{4+} cation is bonded in a distorted body-centered cubic (BCC) geometry to eight (8) equivalent O^{2-} anion atoms. On the other hand, the O^{2-} anion is bonded to four (4) equivalent Zr^{4+} atoms to form a mixture of distorted edge and corner-sharing within the OZr_4 tetrahedral structure where there are four (4) shorter and another four (4) longer Zr–O bond lengths.

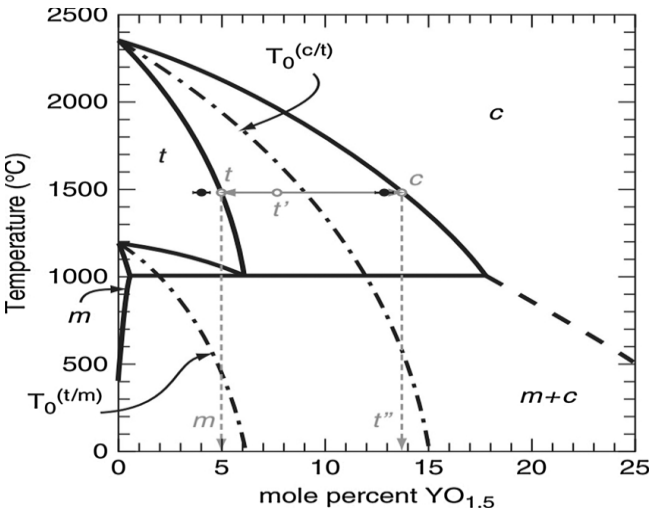

Figure 1: Phase diagram of ZrO_2-Y_2O_3[17].

Table 1: Different phases of ZrO_2[11].

Material	Crystal Structure	Symbol	Space group
ZrO_2	cubic (fluorite)	c-ZrO_2	Fm-3m
	tetragonal	t-ZrO_2	$P4_2/nmc$
	monoclinic (baddeleyite)	m-ZrO_2	$P2_1/c$

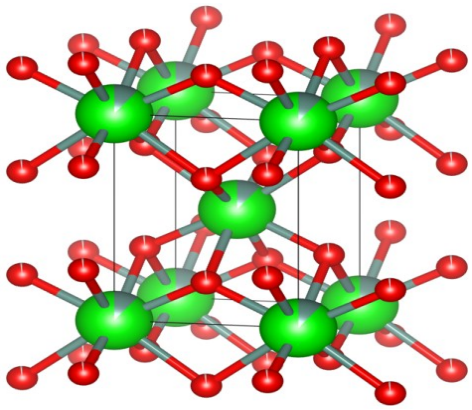

Figure 2: Tetragonal structure of 8YSZ. (Zr/Y: Green, O: Red)

Table 2: Lattice parameters of tetragonal 8YSZ[19].

Crystal. System	a	b	c	α	β	γ	Unit cell volume
Tetragonal	3.6251 Å		5.14 Å	90°			67.547849 A^3

8YSZ with that tetragonal structure is usually named as t'-phase. This t'-YSZ is a metastable phase because it is a supersaturated phase at almost all temperatures range. Moreover, it will decompose into a mixture of Y-lean (t) and Y-rich cubic (c) phases. Furthermore, the remaining exhausted t-phase will transform easily to monoclinic (m) phase during cooling[20].

Interestingly, the Y-rich cubic (c) phase in YSZ has cubic fluorite structure with similar lattice parameters to uranium dioxide (UO_2) which is the main used fuel in nuclear power plants. So, YSZ with cubic crystal structure had been studied extensively due to that similarity in addition to the other wide applications of YSZ in high temperature applications[1, 21-38].

MW sintering of YSZ has been extensively investigated using different types of compositions, microwave cavities such as multimode and single-modes, equipped with various insulation and susceptor types[23, 39-45]. These studies have also explored the sintering behavior where temperature measurements have been conducted using different methods, such as regular thermocouples, optical and/or Infrared (IR) pyrometers with thermal imaging cameras[46, 47]. Additionally, the green samples used in these experiments have varied in initial densities and shapes.

In the current study, HMW sintering of 8YSZ was investigated where the evolution of phases and microstructural changes behavior were studied.

II. Materials and experimental work

The used 8YSZ powder was white in color with the commercial name, Metco 204NS-G, that was manufactured by Oerlikon Metco's Hollow Spherical Powder (HOSP)™ process. The spherical particles were achieved via HOSP when the particles heat up at a temperature that is higher than their melting point allowing the surface tension to pull them into the minimum energy spherical shape at ambient atmosphere. The 8YSZ particles produced by HOSP are used mainly in thermal barrier and/or thermal shock resistance applications. Its melting point is around 2800°C with a normal particle size distribution of (-125 +11) µm. The median diameters are as follows: D 90% from (93 – 103) µm, D 50% from (50 – 57) µm and D 10% from (21 – 25) µm. The chemical composition of the used 8 YSZ powder is shown in table 3 with a maximum of 2.5% of HfO_2 included in the ZrO_2 balance and 6% maximum of monoclinic phase.

Table 3: Chemical composition of 8YSZ powder.

Oxide	ZrO_2	Y_2O_3	SiO_2	TiO_2	Al_2O_3	Fe_2O_3	Othes	Monoclinic Phase
wt.% (max)	rest	7.0 – 8.0	0.05				0.5	6

The powder was pressed into cylindrical shape disks (~30 mm in diameter x 5 mm in height) using uniaxial press machine before it was sintered using HMW processing.

HMW sintering of the prepared 8YSZ pellets was done using a commercial Carbolite LTd microwave (MW) assist box furnace with the model # MRF 16/22/3508P1 that can reach up to 1600°C. This HMW furnace combines both free radiating heating elements using 9 kW molybdenum disilicide heating elements in addition to a microwave radiation source working at 2.45 GHz frequency with 1.8 kW magnetron power. Regular conventional heating elements will heat material from the outside to the inside while the HMW energy will heat the material volumetrically. So, that equipment is using HMW processing concept in a controlled manner, as shown schematically in figure 3.

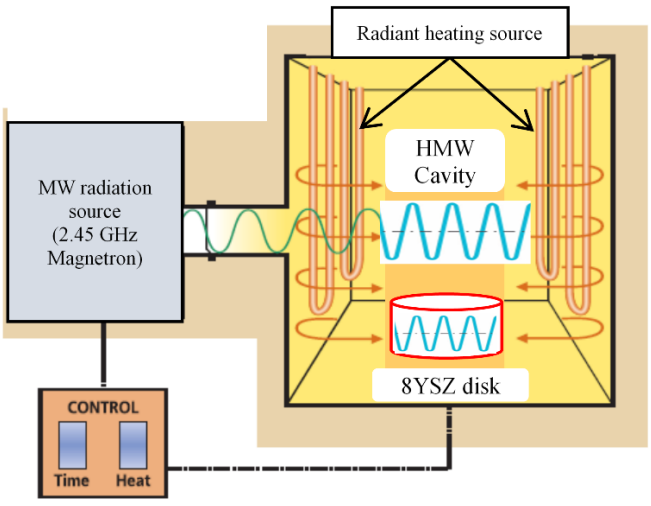

Figure 3: Schematic of HMW setup with combined radiant and MW heating.

The prepared 8YSZ disks was sintered using HMW at 3 different heat-treatment temperatures: 1350

ºC, 1400 ºC and 1450 ºC using a heating rate of 50ºC/min and holding time of 2 hours before being allowed to cool down to room temperature. The sintered disks were characterized using X-ray diffraction (XRD) with Rigaku Miniflex-II Mini-X-ray diffraction machine at 5° min^{-1} rate using Cu Kα source with 0.15406 nm wavelength working at 10mA current and 30kV voltage. Furthermore, the sintered 8YSZ samples were characterized using scanning electron microscopy (SEM) model (FEI Quanta 250) where the disks were platinum coated using a Quorum coating machine model Q150R.

III. Results

SEM of 8YSZ as-received powder is shown in figure 4 with its characteristic spherical shape produced by HOSP process.

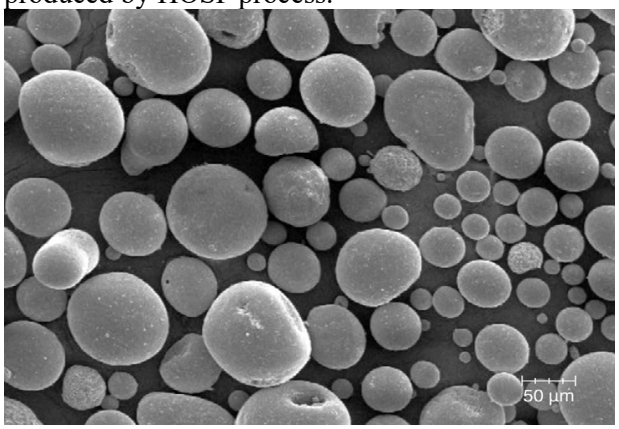

Figure 4: SEM of the as-received 8%YSZ.

The XRD patterns of the as-received 8YSZ sample and the corresponding sintered samples using HMW heating at three (3) different temperatures (1350 ºC, 1400 ºC and 1450 ºC) are shown in figure 5. The as-received XRD pattern of 8YSZ powder shows that the addition of 7-8 wt.% of Y_2O_3 has stabilized the metastable tetragonal crystal structure in the (t'-ZrO_2) phase with a residual minor portion of the monoclinic (m-ZrO_2) phase, as indicated in the chemical composition of the powder shown in table 3 and matched with other previous studies[17, 48, 49]. The major XRD peaks were indexed and identified as tetragonal crystal structure with ICDD PDF-card # 01-070-4432. The existence of the detected minor portion of (m-ZrO_2) phase is due to the local inhomogeneity in the used commercial 8YSZ powder with its coarser microstructure in the micrometric size which will cause higher strains during cooling, as shown in other studies[50, 51]. In addition, the XRD patterns of heated-treated samples using HMW had also shown existence of a mixture of the residual of unstable tetragonal (t'-ZrO_2), stable tetragonal (t-ZrO_2) phase, cubic phase (c-ZrO_2) and traces of monoclinic (m-ZrO_2) phase, as will be discussed in the following section.

In order to show this mixture of phases, figures 6 and 7 are showing two selected 2θ ranges of the HMW heat-treated samples from (27-33) and from (72-77), respectively. As shown in figure 6, the amount of the detected (m-ZrO_2) phase in all the three HMW heat-treated samples was decreasing in amount, compared to the as-received powder where it was continuously decreasing as the temperature was increasing from 1350 ºC till 1450 ºC.

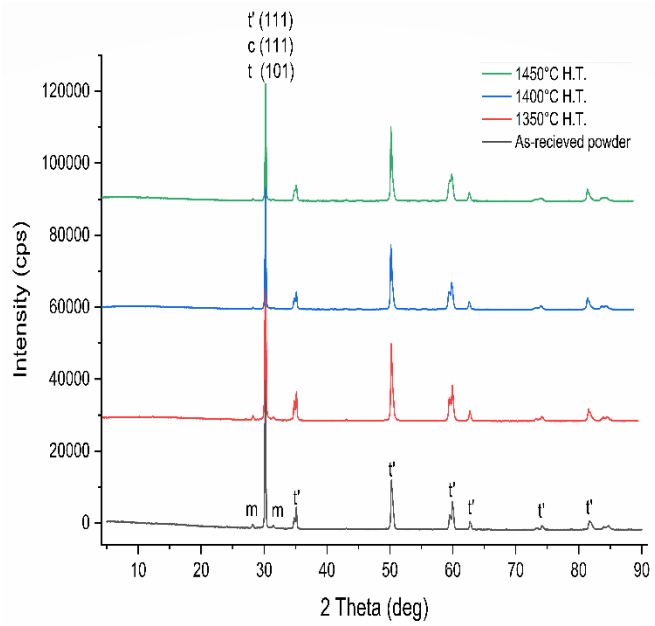

Figure 5: XRD of the as-received 8%YSZ and the HMW heat-treated corresponding samples at different temperatures.

Furthermore, another critical change was noticed related to the decomposition of the metastable tetragonal (t'-ZrO_2) phase where the changes in the XRD peaks of (400) and (004) plans as a function of sintering temperature is shown in figure 7. As the temperature increases from 1350 ºC to 1450 ºC, the evaluation of a new peak related to the cubic (c-ZrO_2) phase is observed first at 1350ºC sample then become more obvious as the temperature increases to 1450ºC. The peaks slightly shift toward larger angles due to a decrease in the lattice parameter caused by MW heating[52]. The metastable non-transformable (t'-ZrO_2) phase had started to decompose gradually into

the stable transformable tetragonal (t-ZrO_2) phase with low yttria content and the other stable cubic-(c-ZrO_2) phase[53]. The cubic phase was identified and matched well with ICDD PDF-card #01-030-1468. The stable tetragonal phase (t-ZrO_2) is restricted to the solubility limit while the unstable tetragonal phase (t'-ZrO_2) has an expanded solubility limit but decomposes into a mixture of the stable tetragonal and cubic phases[54], as confirmed from the equilibrium phase diagram, shown in figure 1.

Usually under normal conventional heating above ~1300ºC, followed by cooling to RT, the developed stable tetragonal-t phase will subsequently transform into the monoclinic-m phase (m-ZrO_2), causing an increase of ~3–5% in volume with a major deterioration in the mechanical properties due to extensive microcracking[55], so this transformation of t into m phases is not desired.

As shown in figures 6 & 7, HMW heating was allowing the decomposition of the metastable tetragonal (t'-ZrO_2) phase into both the stable cubic (c-ZrO_2) and tetragonal (t-ZrO_2) phases while suppressing the subsequent martensitic transformation of (t-ZrO_2) phase into (m-ZrO_2) phase. Hence, decreasing the amount of (m-ZrO_2) phase as the temperature increases to 1450ºC. One reason could explain why HMW heating had suppressed this phase transformation might be due to the formation of high number of anion vacancies in 8 YSZ samples during microwave heat-treatment where the increase in oxygen vacancies will act as a stabilizer for the cubic phase[52]. So, the high amount of oxygen vacancies formation induced by microwave irradiation followed by air cooling to RT will cause the formed extra oxygen vacancies to displace the oxygen ions from its equilibrium position in the tetragonal phase and act as a cubic phase stabilizer and consequently the martensitic transformation was suppressed[52, 56]. Therefore, sintering of 8 YSZ using HMW processing will be more attractive than conventional heating.

The average crystallites sizes of the three HMW sintered 8YSZ samples were calculated to be around 46-49 nm using Scherrer equation as follows:

$$\beta = \frac{k\,\lambda}{L\cos\theta}$$

Where β is the full width at half-maximum (FWHM) of the diffraction peak in radians, L is crystalline size in (Å), k = 0.92, θ is the Bragg angle and λ = 1.5406 Å.

SEM micrographs of the sintered 8YSZ samples using HMW heating at 1350 ºC, 1400 ºC and 1450 ºC, respectively, are shown in figure 8. The figure indicates the closer of major pores between spherical powder particles during MW sintering with the formation of well defined-grain boundaries which indicating the successful sintering of 8YSZ samples. Furthermore, the average grain size was slowly and gradually increasing from 46 µm till 49 µm, as confirmed using XRD calculation, as the temperature was increasing from 1350 ºC till 1450 ºC. The shown minor observed voids might be due to possible spherical particle displacement or collapsing of particles during HMW sintering.

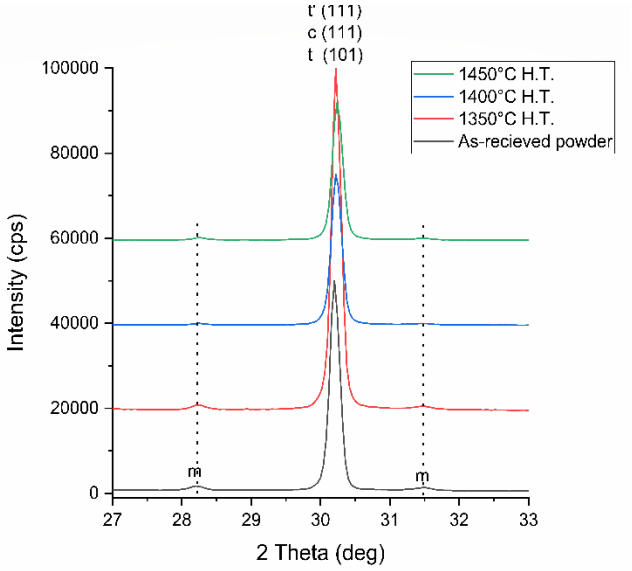

Figure 6: XRD of samples for 2θ range 27-33.

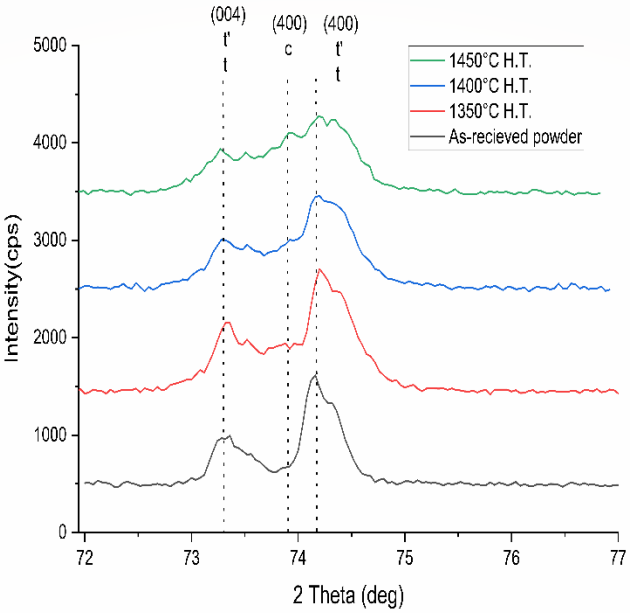

Figure 7: XRD of samples for 2θ range from 72-77.

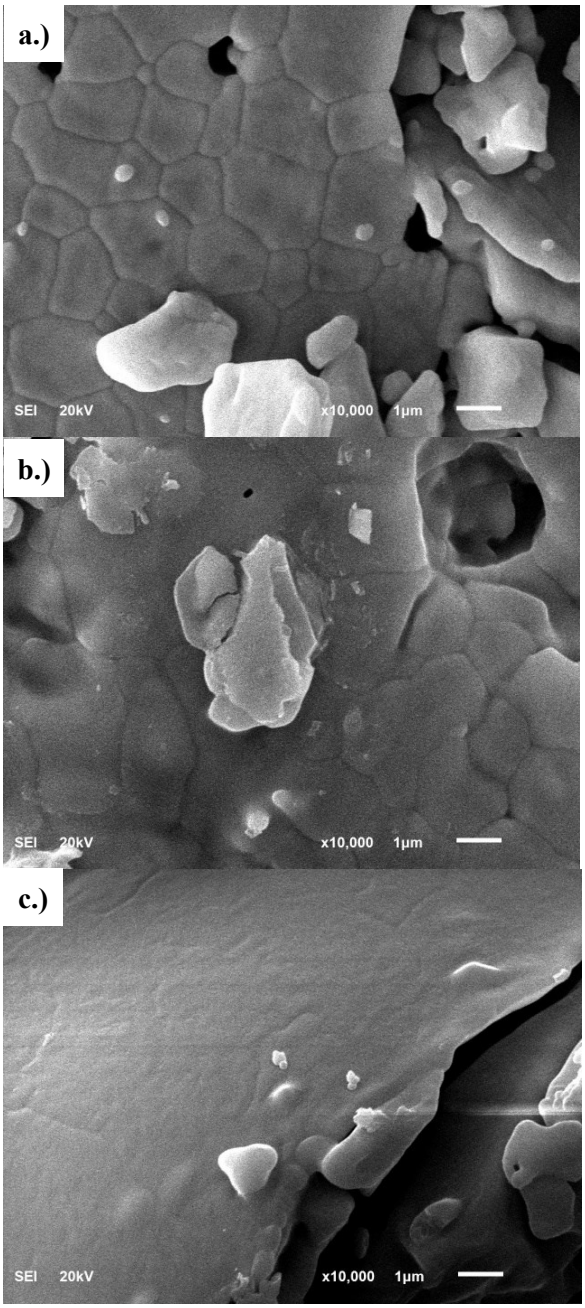

Figures 8: SEM of 8YSZ sintered samples using HMW heating at 1350 ºC (a), 1400 ºC (b) and 1450 ºC (c), respectively.

IV. Conclusions

Sintering of 8YSZ was successfully achieved using HMW processing. Phase decomposition, transformation, and microstructural changes during HMW heat-treatment of 8YSZ at 3 different temperatures were discussed. HMW had been found to allow the decomposition of non-transformable metastable tetragonal (t'-ZrO_2) phase into the transformable tetragonal and cubic phases. Furthermore, HMW heat-treatment of 8YSZ was found to suppress the regular phase transformation of the formed stable tetragonal (t-ZrO_2) phase into the monoclinic (m-ZrO_2) phase due to the formation of vast number of anion vacancies generated during the molecular heating of microwave radiation followed by air cooling. The MW generated substantial number of defects and vacancies will act as a stabilizer for the cubic (c-ZrO_2) phase, preventing the common crack-induced martensite transformation of (t into m) as an undesired transformation that usually causes degradation in the material mechanical properties. Consequently, sintering of 8 YSZ using HMW processing is more attractive than conventional heating. HMW heat-treated sample at 1450ºC has shown the most clear and obvious cubic phase peak formation in the 2θ range between ~73-74. Hybrid microwave processing is considered as a promising technique to sinter YSZ materials, consequently HMW is a promising candidate to process nuclear materials such as uranium dioxide (UO_2) due to its structural similarity (fluorite structure) to cubic (c-ZrO_2) phase.

Acknowledgments

I would like to thank the Deanship of Research Oversight and Coordination (DROC) at King Fahd University of Petroleum and Minerals (KFUPM) for funding this work with the grant DF191054. I acknowledge the support of the Interdisciplinary Research Center for Advanced Materials (IRC-AM) at KFUPM. I am grateful to Mechanical Engineering Department for their continuous support.

References

1. Yin, Y., et al., *A critical review on sintering and mechanical processing of 3Y-TZP ceramics.* Ceramics International, 2023. **49**(2): p. 1549-1571.
2. Singh, C., V. Khanna, and S. Singh, *Sustainability of microwave heating in materials processing technologies.* Materials Today: Proceedings, 2023. **73**: p. 241-248.
3. Sutton, W., *Microwave processing of ceramic materials.* American Ceramic Society Bulletin, 1989.
4. Wilson, J. and S.M. Kunz, *Microwave Sintering of Partially Stabilized Zirconia.* Journal of the American Ceramic Society, 1988. **71**(1): p. C-40-C-41.
5. Wroe, R. and A.T. Rowley, *Evidence for a non-thermal microwave effect in the sintering of*

partially stabilized zirconia. Journal of Materials Science, 1996. **31**(8): p. 2019-2026.

6. Binner, J., *Microwave processing of materials: London, 12 April 1991.* Materials & Design, 1991. **12**(4): p. 231-231.
7. Clark, D.E. and W.H. Sutton, *Microwave processing of materials.* Annual Review of Materials Science, 1996. **26**: p. 299-331.
8. Metaxas, A.C. and R.J. Meredith, *Industrial Microwave Heating*. 1983, London,UK: Peregrinus.
9. Clark, D.E., et al., *Microwave Solutions for Ceramic Engineers*. 2006.
10. Menezes, R.R., P.M. Souto, and R. Kiminami, *Microwave hybrid fast sintering of porcelain bodies.* Journal of Materials Processing Technology, 2007. **190**(1-3): p. 223-229.
11. STUBICAN, V.S., R.C. HINK, and S.P. RAY, *Phase Equilibria and Ordering in the System ZrO2-Y2O3.* Journal of the American Ceramic Society, 1978. **61**(1-2): p. 17-21.
12. HEUER, A.H., et al., *Stability of Tetragonal ZrO2 Particles in Ceramic Matrices.* Journal of the American Ceramic Society, 1982. **65**(12): p. 642-650.
13. MAZDIYASNI, K.S., C.T. LYNCH, and J.S.S. II, *Cubic Phase Stabilization of Translucent Yttria-Zirconia at Very Low Temperatures.* Journal of the American Ceramic Society, 1967. **50**(10): p. 532-537.
14. Witz, G., et al., *Phase Evolution in Yttria-Stabilized Zirconia Thermal Barrier Coatings Studied by Rietveld Refinement of X-Ray Powder Diffraction Patterns.* Journal of the American Ceramic Society, 2007. **90**(9): p. 2935-2940.
15. Elbakhshwan, M.S. and B.J. Heuser, *Structural and compositional characterization of single crystal uranium dioxide thin films deposited on different substrates.* Thin Solid Films, 2017. **636**: p. 658-663.
16. Zhou, G., et al., *X-ray diffraction analysis of the yttria stabilized zirconia powder by mechanical alloying and sintering.* Ceramics International, 2020. **46**(7): p. 9691-9697.
17. Lipkin, D.M., et al., *Phase Evolution upon Aging of Air-Plasma Sprayed t′-Zirconia Coatings: I—Synchrotron X-Ray Diffraction.* Journal of the American Ceramic Society, 2013. **96**(1): p. 290-298.
18. Lima, R.S., *Perspectives on Thermal Gradients in Porous ZrO2-7–8 wt.% Y2O3 (YSZ) Thermal Barrier Coatings (TBCs) Manufactured by Air Plasma Spray (APS).* Coatings, 2020. **10**(9): p. 812.
19. Lamas, D.G. and N.E.W.D. Reca, *X-ray diffraction study of compositionally homogeneous, nanocrystalline yttria-doped zirconia powders.* Journal of Materials Science, 2000. **35**(22): p. 5563-5567.
20. Bai, M., et al., *Microstructure and phase stability of suspension high velocity oxy-fuel sprayed yttria stabilised zirconia coatings from aqueous and ethanol based suspensions.* Journal of the European Ceramic Society, 2018. **38**(4): p. 1878-1887.
21. Lai, Q., et al., *Cold sintering process assisted sintering for 8YSZ ceramic: A way of achieving high density and electrical conductivity at a reduced sintering temperature.* Ceramics International, 2023.
22. Kumari, N., et al., *Synthesis of low-band gap porous zirconia nanoparticles via greener-route: Mechanistic investigation and their applications.* Materials Chemistry and Physics, 2023. **294**: p. 127004.
23. Huang, W., et al., *Research on the tetragonal phase content and microstructure of microwave-assisted sintering Y-PSZ system doped Bi2O3.* Journal of Materials Research and Technology, 2023.
24. Chen, X., et al., *Effect of Zr4+ substitution on the phase evolution and microwave dielectric properties of (Cu1/3Nb2/3)0.25Ti0.75-xZrxO2 ceramics.* Ceramics International, 2023. **49**(3): p. 5022-5028.
25. Zhong, Z., et al., *Microwave sintering of high-performance BaZr0.1Ce0.7Y0.1Yb0.1O3-δ (BZCYYb) electrolytes for intermediate-temperature solid oxide fuel cells.* International Journal of Hydrogen Energy, 2022. **47**(60): p. 25367-25377.
26. Zhong, S., et al., *High-performance zirconia ceramic additively manufactured via NanoParticle Jetting.* Ceramics International, 2022. **48**(22): p. 33485-33498.
27. Zhang, Y., et al., *Ball milling assisted preparation of nano La–Y/ZrO2 powder ternary oxide system: Influence of doping amounts.* Ceramics International, 2022.
28. Xu, X., et al., *Modified room temperature solid-state synthesis of yttria-stabilized zirconia (YSZ) nano-powders for solid oxide fuel cells.* Journal of Rare Earths, 2022.
29. Wu, Y., et al., *High-surface-area mesoporous silica-yttria-zirconia ceramic materials prepared by coprecipitation method — the role of silicon.* Ceramics International, 2022. **48**(15): p. 21951-21960.
30. Varghese Kurian, J., et al., *Effect of material characteristics on thermal, tribological and mechanical properties of high temperature cast iron coatings.* Materials Today: Proceedings, 2022. **65**: p. 3629-3641.

31. Sktani, Z.D.I., et al., *Effects of additives additions and sintering techniques on the microstructure and mechanical properties of Zirconia Toughened Alumina (ZTA): A review.* International Journal of Refractory Metals and Hard Materials, 2022. **106**: p. 105870.
32. Sarker, S., et al., *Impacts of inclusion of additives on physical, microstructural, and mechanical properties of Alumina and Zirconia toughened alumina (ZTA) ceramic composite: A review.* Materials Today: Proceedings, 2022. **62**: p. 2892-2918.
33. Sara Lee, K.Y., et al., *Low-temperature degradation behaviour of microwave sintered CuO-doped Y-TZP ceramics.* Materials Today: Proceedings, 2022. **66**: p. 2791-2795.
34. Rua Taborda, M.I., et al., *A new chemical pathway towards densification of tetragonal zirconia below 900 °C.* Materialia, 2022. **24**: p. 101479.
35. Rada, S., et al., *Advanced zirconia ceramics stabilized with yttria and magnesia: Structure and Vickers microhardness.* Journal of the Mechanical Behavior of Biomedical Materials, 2022. **134**: p. 105425.
36. Moratal, S., et al., *Microwave sintering study of strontium-doped lanthanum manganite in a single-mode microwave with electric and magnetic field at 2.45 GHz.* Journal of the European Ceramic Society, 2022. **42**(13): p. 5624-5630.
37. Manière, C., et al., *Flash spark plasma sintering of zirconia nanoparticles: Electro-thermal-mechanical-microstructural simulation and scalability solutions.* Journal of the European Ceramic Society, 2022. **42**(1): p. 216-226.
38. Liu, L., et al., *Solvothermal synthesis of zirconia nanomaterials: Latest developments and future.* Ceramics International, 2022. **48**(22): p. 32649-32676.
39. Chaix, J.-M., *Microwave Sintering of Ceramics*, in *Encyclopedia of Materials: Technical Ceramics and Glasses*, M. Pomeroy, Editor. 2021, Elsevier: Oxford. p. 327-341.
40. Chen, G., et al., *Stability properties and structural characteristics of CaO-partially stabilized zirconia ceramics synthesized from fused ZrO2 by microwave sintering.* Ceramics International, 2020. **46**(10, Part B): p. 16842-16848.
41. Croquesel, J., et al., *Design of an instrumented microwave multimode cavity for sintering of nuclear ceramics.* Materials & Design, 2021. **204**: p. 109638.
42. Garnault, T., et al., *Is direct microwave heating well suited for sintering ceramics?* Ceramics International, 2021. **47**(12): p. 16716-16729.
43. Gil-Flores, L., et al., *Microstructure and mechanical properties of 5.8 GHz microwave-sintered ZrO2/Al2O3 ceramics.* Ceramics International, 2019. **45**(14): p. 18059-18064.
44. Khalile, N., et al., *Microwave sintering of dense and lattice 3Y-TZP samples shaped by digital light processing.* Ceramics International, 2022.
45. Khalile, N., et al., *Hybrid microwave sintering of alumina and 3 mol% Y2O3-stabilized zirconia in a multimode cavity – Influence of the sintering cell.* Ceramics International, 2022. **48**(13): p. 18143-18150.
46. Chen, Y., et al., *Microwave sintering and fracture behavior of zirconia ceramics.* Ceramics International, 2019. **45**(14): p. 17675-17680.
47. Ramesh, S., et al., *Comparison between microwave and conventional sintering on the properties and microstructural evolution of tetragonal zirconia.* Ceramics International, 2018. **44**(8): p. 8922-8927.
48. Poliarus, O., et al., *Microstructure, mechanical and thermal properties of YSZ thermal barrier coatings deposited by axial suspension plasma spraying.* Archives of Civil and Mechanical Engineering, 2023. **23**(2): p. 89.
49. Krogstad, J.A., et al., *Phase Evolution upon Aging of Air Plasma Sprayed t′-Zirconia Coatings: II−Microstructure Evolution.* Journal of the American Ceramic Society, 2013. **96**(1): p. 299-307.
50. Vaßen, R., *Thermal Barrier Coatings*, in *Ceramics Science and Technology*. 2013. p. 95-115.
51. Patterson, T., et al., *Thermal cyclic lifetime and oxidation behavior of air plasma sprayed CoNiCrAlY bond coats for thermal barrier coatings.* Surface and Coatings Technology, 2008. **203**(5): p. 437-441.
52. Moon, J., et al., *The effects of heat treatment on the phase transformation behavior of plasma-sprayed stabilized ZrO2 coatings.* Surface and Coatings Technology, 2002. **155**(1): p. 1-10.
53. Taylor, R., J.R. Brandon, and P. Morrell, *Microstructure, composition and property relationships of plasma-sprayed thermal barrier coatings.* Surface and Coatings Technology, 1992. **50**(2): p. 141-149.
54. Lima, R.S. and B.R. Marple, *Insights on the High-Temperature Operational Limits of ZrO₂-Y₂O₃ TBCs Manufactured via Air Plasma Spray.* Journal of Materials Engineering and Performance, 2017. **26**: p. 1272-1282.
55. Riva, V., et al., *Insight into t->m transition of MW treated 3Y-PSZ ceramics by grazing incidence X-ray diffraction.* Journal of the European Ceramic Society, 2022. **42**(1): p. 227-237.
56. Green, D.J., *Transformation Toughening Of Ceramics (1st ed.)*. 1989: CRC Press.